Journal of the Ceramic Society of Japan 117 [5] 693-697 2009 Paper

Effect of Bi_2O_3 addition and sintering time on the physical and electrical properties of lead-free $(Na_{0.5}Bi_{0.5})TiO_3$–$Ba(Zr_{0.04}Ti_{0.96})O_3$ ceramics

Chun-Huy WANG†

Department of Electronic Engineering, Nan-Jeon Institute of Technology, Tainan, Taiwan 737, R.O.C.

Although $PbZrO_3$–$PbTiO_3$ (PZT)-based ceramics are playing a dominant role in piezoelectric materials, their evaporation of harmful lead oxide during the sintering process causes a crucial environment problem. It is necessary to search for lead-free piezoelectric materials that have such excellent properties as those found in the PZT-based ceramics. Therefore $(Na_{0.5}Bi_{0.5})TiO_3$-based solid solutions were studied to improve piezoelectric properties. In the present study, various quantities of Bi_2O_3 were added into $0.99(Na_{0.5}Bi_{0.5})TiO_3$–$0.01Ba(Zr_{0.04}Ti_{0.96})O_3$ (0.99NBT–0.01BZT) ceramics. High-density samples were obtained through the addition of Bi_2O_3 into 0.99NBT–0.01BZT ceramic. It was found that 0.99NBT–0.01BZT with the addition of 0–4.0 wt% Bi_2O_3 exhibit relatively good piezoelectric properties. For 0.99NBT–0.01BZT ceramic with the addition of 0.5 wt% Bi_2O_3, the electromechanical coupling coefficients of the planar mode k_p and the thickness mode k_t reach 0.15 and 0.55, respectively, at the sintering of 1100°C for 2 h. The ratio of thickness coupling coefficient to planar coupling coefficient is 3.6. It is obvious that 0.99NBT–0.01BZT solid solution ceramic by adding low quantities of Bi_2O_3 is one of the promising lead-free ceramics for high frequency electromechanical transducer applications.

©2009 The Ceramic Society of Japan. All rights reserved.

Key-words : Lead-free piezoceramics, Piezoelectric property, Crystal structure, Dielectric property

[Received December 1, 2008; Accepted February 19, 2009]

1. Introduction

The market for piezoceramic components is dominated by lead-based PZT materials containing more than 60 wt% lead. In as much as lead is highly toxic, it has become a great concern how to eliminate the use of PZT by replacing it by non-harmful materials while maintaining comparable electrical properties. Due to the increasing demand for environmental protection, studies have been performed in depth on various lead-free ceramics for environmentally friendly applications. The search for alternative piezoelectric materials is now being focused on alkali noibates, modified bismuth titanates, etc. Among these materials, similar to $(Na_{0.5}Bi_{0.5})TiO_3$ (abbreviated as NBT)-based materials have the perovskite structure, and these materials show excellent properties such as relatively high piezoelectric properties. Perovskite structure NBT ceramic reported by Smolensky et al.[1] is considered as the one of the candidates for lead-free piezoelectric ceramics because of its strong ferroelectric properties and high Curie temperature (T_C = 320°C). At room temperature, NBT ceramic is strongly ferroelectric with a relatively large remnant polarization and large coercive field of 70 kV/cm.

Some modifications of NBT ceramic have proved to be helpful by forming solid solution with other perovskite oxides,[2)–7)] such as $CaTiO_3$,[2)] $BaTiO_3$,[3)] $La_{0.01}TiO_3$,[4)] $BiScO_3$,[5)] $(Sr_{0.5}Ca_{0.5})TiO_3$,[6)] $(Bi_{0.5}K_{0.5})TiO_3$,[7)] etc. Many studies show that the substitution of Ti^{4+} in $BaTiO_3$ with quadrivalence ions (such as Zr^{4+}) can significantly improve the overall properties of the material.[8)] For example, $Ba(Zr_xTi_{1-x})O_3$ (BZT) has a small leakage current as a result of its better chemical stability of Zr^{4+} than Ti^{4+}. The author[9)] previously reported that $0.95(Na_{0.5}Bi_{0.5})TiO_3$–$0.05Ba(Zr_{0.04}T_{i0.96})O_3$ ceramics near the MPB has a good planar coupling factor (k_p = 0.34). The author[9)] reported that $0.99(Na_{0.5}Bi_{0.5})TiO_3$–$0.01Ba(Zr_{0.04}T_{i0.96})O_3$ ceramics exhibit a large anisotropy in the electromechanical coupling factor k_t/k_p (k_t = 0.51, k_p = 0.14) for high frequency electromechanical transducer applications. The comparison of properties of $(Na_{0.5}Bi_{0.5})TiO_3$ ceramics based on the previous reports of various groups are demonstrated in **Table 1**.

For the most important perovskite PZT family, Bi_2O_3 has been common used as an additive to improve their physical and electric properties. Some studies[10)] have reported the effect of excess Bi_2O_3 on the properties of NBT ceramic and demonstrated that Bi_2O_3 doping could enhance the physical and electrical properties of the ceramic. The aim of this study is not only to investigate the physical and electrical properties of $(1-x)(Na_{0.5}Bi_{0.5})TiO_3$–$xBa(Zr_{0.04}T_{i0.96})O_3$ ceramics with an addition of excess Bi_2O_3, but also to fabricate large anisotropy in the

Table 1. Comparison of Properties of $(Bi_{0.5}Na_{0.5})TiO_3$ Ceramics Based on the Previous Reports of Various Groups

Composition	K^T_{33}	k_p (%)	k_t (%)	k_t/k_p	Ref.
$0.99BNT–0.01CaTiO_3$	236	37.6	51.3	1.36	2
$0.94BNT–0.06BaTiO_3$	560	28	49	1.75	3
$0.98BNT–0.02BiScO_3$	431	14.4	–	–	5
$0.87BNT–0.13(Sr_{0.5}Ca_{0.5})TiO_3$	583	12	30	2.5	6
$0.8BNT–0.2(Bi_{0.5}K_{0.5})TiO_3$	1030	27	42	1.56	7
$0.99BNT–0.01Ba(Ti_{0.96}Zr_{0.04})O_3$	553	14	51	3.6	9

† Corresponding author: C.-H. Wang; E-mail: wch70982@ms41.hinet.net

electromechanical coupling factor k_t/k_p for high frequency electromechanical transducer applications. The effect of sintering time on the physical and electrical properties of $(1-x)(Na_{0.5}Bi_{0.5})TiO_3$–$xBa(Zr_{0.04}T_{i0.96})O_3$ ceramics is also discussed.

2. Experimental procedure

The $(1-x)(Na_{0.5}Bi_{0.5})TiO_3$–$xBa(Zr_{0.04}Ti_{0.96})O_3$ (abbreviated $(1-x)$NBT–xBZT) ceramics were prepared by a solid-state reaction method. Additive amounts of Bi_2O_3 were added to the host NBT–BZT ceramic powders in concentration varying from 0 to 4.0 wt%.

Starting materials were Bi_2O_3, Na_2CO_3, $BaCO_3$, TiO_2, ZrO_2 with purities of at least 99.5% and weighted according to the stoichiometric composition (x = 0.01, 0.03, 0.05, 0.07 0.09 and 0.11). Bi_2O_3 was added after the calcination at 900°C for 2 h. The calcined powders were pressed (CIP) at 180 MPa into pellets with 15 mm in diameter. The disc samples were sintered in aluminum crucible at 1100°C for 2–8 h in an air atmosphere. To measure relevant piezoelectric properties, the prepared ceramic samples were polarized in silicone oil at 100°C under the electric field of 4 kV/mm for 30 min. An X-ray diffractometer (Seimens D5000) using Cu Kα radiation was used to evaluate the crystal structure of the sintered ceramics. The room temperature dielectric constant at 1 kHz was measured by an LCR meter (Angilent 4284A). The piezoelectric properties were measured by a resonance-antiresonance method based on IEEE standards[11] using an impedance/gain-phase analyzer (Angilent 4194). Samples for observations of the microstructure were polished and thermal etched. The microstructures were observed by a scanning electron microscope (SEM). The mean grain size was calculated by the line intercept method.[12] The density was measured by Archimedes method.

3. Results and discussion

Figures 1 to 5 show the physical and electrical properties of $(1-x)(Na_{0.5}Bi_{0.5})TiO_3$–$xBa(Zr_{0.04}Ti_{0.96})O_3$ (x = 0.01, 0.03, 0.05, 0.07, 0.09 and 0.11) sintered for different time at 1100°C. According to the author's previous report,[9] the MPB of $(1-x)$NBT–xBZT system ceramic lies in the composition range of $0.05 \le x \le 0.07$ at room temperature, where hexagonal and tetragonal phases coexist. The materials with perovskite structure are hexagonal phase at $x \le 0.05$ and become tetragonal phase at $x \ge 0.07$. The measured density of $(1-x)$NBT–xBZT ceramic is shown as function of BZT composition and sintering time in Fig. 1. The measured density of the sintered samples is 92–96% of the theoretical density for 5 h at 1100°C. In general, the measured density increases with an increase of BZT addition until it reaches a maximum value at the phase boundary (x = 0.05), then decreases for higher BZT addition. **Figure 2** shows the microstructure of $(1-x)(Bi_{0.5}Na_{0.5})TiO_3$–$xBa(Ti_{0.96}Zr_{0.04})O_3$ ceramics for different x compositions at the sintering of 1100°C for 5 h. The $0.95(Bi_{0.5}Na_{0.5})TiO_3$–$0.05Ba(Ti_{0.96}Zr_{0.04})O_3$ ceramic is more dense, with low porosity, and grain size of ~1.5 μm in Fig. 2(c).The reason for the maximum value of the density at the phase boundary is considered as the existence of the DSR (different symmetry regions). The DSR means the regions of the tetragonal phase are in the hexagonal grains and the regions of the hexagonal phase are in tetragonal grains. It may be explained by the sintering model of Coble[13] that the existence of the DSR will offer the interphase boundary as a sink of defect or vacancy resulting in the increase of the density. The measured density increases with an increase sintering time until it reaches 5 h, then decreases for 8 h.

The poled dielectric constant K^T_{33} of $(1-x)$NBT–xBZT ceramic are shown as function of BZT composition and sintering time in **Fig. 3**. The dielectric constant K^T_{33} increases with increasing sintering time until it reaches 5 h, then decreases above 8 h. The highest planar coupling factor (K^T_{33} = 1020) of $(1-x)$NBT–xBZT ceramic is found at x = 0.07. As far as dielec-

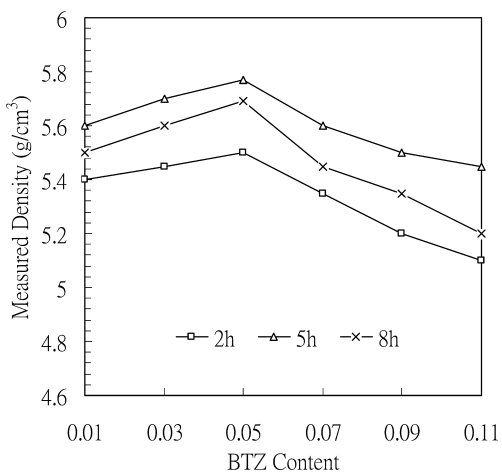

Fig. 1. Measured density of $(1-x)(Bi_{0.5}Na_{0.5})TiO_3$–$xBa(Ti_{0.96}Zr_{0.04})O_3$ ceramics sintered 1100°C as functions of BZT content and sintering time.

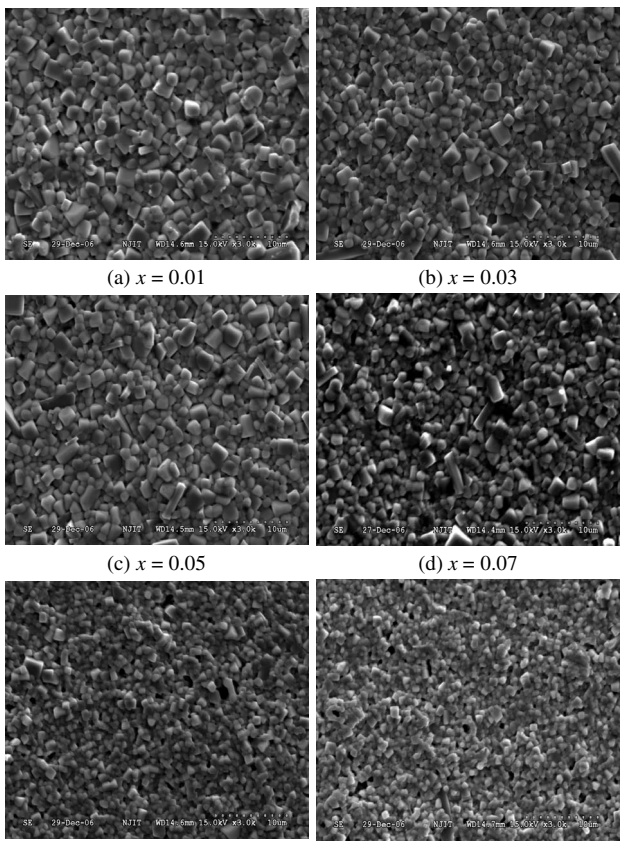

(a) x = 0.01 (b) x = 0.03 (c) x = 0.05 (d) x = 0.07 (e) x = 0.09 (f) x = 0.11

Fig. 2. SEM images of $(1-x)(Bi_{0.5}Na_{0.5})TiO_3$–$xBa(Ti_{0.96}Zr_{0.04})O_3$ ceramics for different x compositions: (a) x = 0.01, (b) x = 0.03, (c) x = 0.05, (d) x = 0.07, (e) x = 0.09, and (f) x = 0.11.

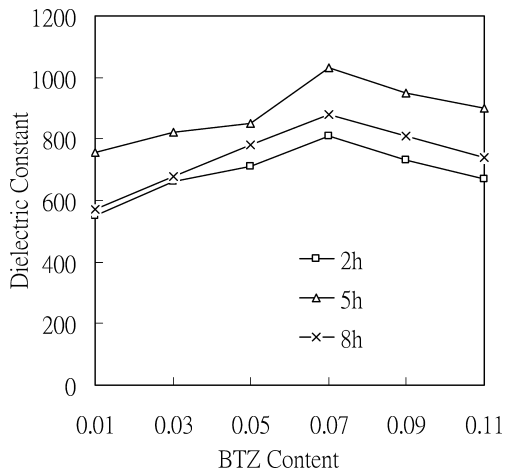

Fig. 3. Dielectric constant of $(1-x)(Bi_{0.5}Na_{0.5})TiO_3$–$xBa(Ti_{0.96}Zr_{0.04})O_3$ ceramics sintered 1100°C as functions of BZT content and sintering time.

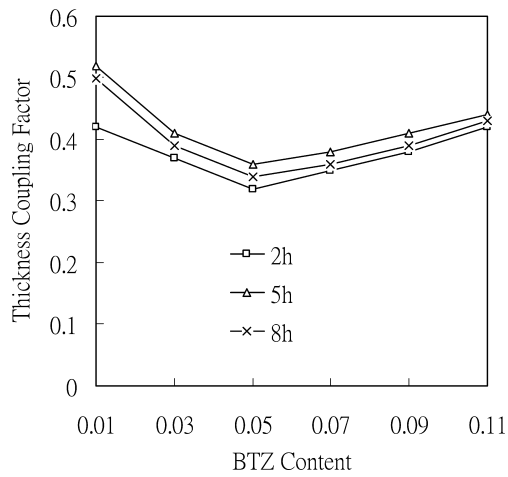

Fig. 5. Thickness coupling factor of $(1-x)(Bi_{0.5}Na_{0.5})TiO_3$–$xBa(Ti_{0.96}Zr_{0.04})O_3$ ceramics sintered 1100°C as functions of BZT content and sintering time.

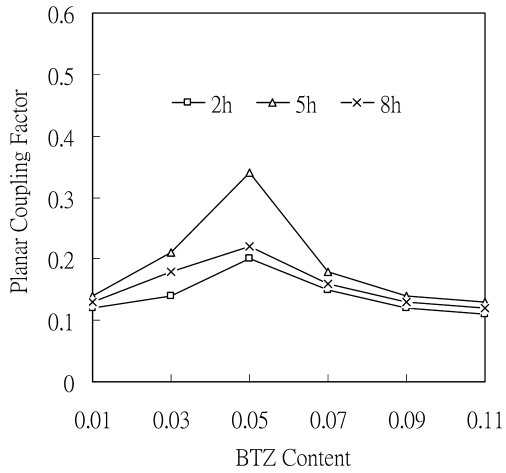

Fig. 4. Planar coupling factor of $(1-x)(Bi_{0.5}Na_{0.5})TiO_3$–$xBa(Ti_{0.96}Zr_{0.04})O_3$ ceramics sintered 1100°C as functions of BZT content and sintering time.

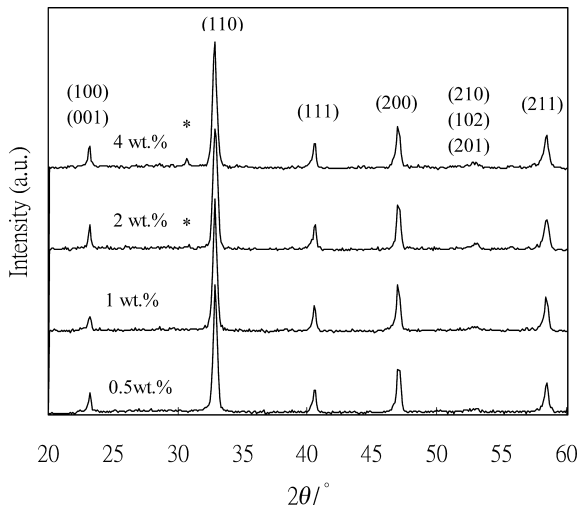

Fig. 6. XRD Patterns of $0.99(Bi_{0.5}Na_{0.5})TiO_3$–$0.01Ba(Ti_{0.96}Zr_{0.04})O_3$ ceramics sintered 1100°C for 2 h with different Bi_2O_3 addition: (a) 0.5 wt%, (b) 1 wt%, (c) 2 wt%, and (d) 4 wt%.

tric constant of polarized ceramic is concerned, its maximum in multi-component systems is displaced into tetragonal phase and does not coincide with the maximum of electromechanical coupling factor. The reasons of displacement of maximum K^T_{33} into tetragonal phase can be explained by Fesenko et al.[14)]

The planar coupling factor (k_p) and thickness coupling factor (k_t) of $(1-x)$NBT–xBZT ceramic are shown as function of BZT composition and sintering time in **Fig. 4** and **Fig. 5**. Until the sintering time rises to 5 h, the k_p and the k_t gradually increase. However, after 5 h, the k_p and the k_t gradually decrease, probably because of a lower density. The electromechanical coupling factor, k, is related to different BZT addition. The k has been used extensively as a measure of the piezoelectric response of PZT type ceramics. It was found that the k depended on the material parameters[15)] such as grain size, porosity, and chemical composition. Piezoelectric activity reaches a maximum, when ceramic compositions are chosen near those of the morphotropic phase boundary. Usually, the piezoelectric activity is appreciated by the value of the electromechanically coupling factor in radial mode k_p. Therefore, k_p is the figure of merit of the piezoelectric activity and the square of that gives the efficiency of the conversion of electrical-mechanical energy.[16)] Usually, the piezoelectric activity increases with the value of the electromechanical coupling factor in radial mode k_p. The highest planar coupling factor (k_p = 0.34) is found at the phase boundary (x = 0.05). The highest thickness coupling factor (k_t = 0.51) is found at x = 0.01. For $0.99(Na_{0.5}Bi_{0.5})TiO_3$–$0.01Ba(Zr_{0.04}Ti_{0.96})O_3$ (abbreviated 0.99NBT–0.01BZT) ceramics, the electromechanical coupling coefficients of the planar mode k_p and the thickness mode k_t reach 0.14 and 0.51, respectively, at the sintering of 1100°C for 5 h. The ratio of thickness coupling coefficient to planar coupling coefficient is 3.6. The 0.99NBT–0.01BZT ceramic exhibits a large anisotropy in the electromechanical coupling factor k_t/k_p for high frequency electromechanical transducer applications.

Figure 6 shows the XRD patterns of $0.99(Na_{0.5}Bi_{0.5})TiO_3$–$0.01Ba(Zr_{0.04}Ti_{0.96})O_3$ ceramics system with different Bi_2O_3 addition sintered 1100°C for 2 h. The hexagonal symmetry of 0.99NBT–0.01BZT ceramic at room temperature was found on the XRD patters. A small amount of the second phase appears in the 2θ ranges of 30–32° for higher Bi_2O_3 addition (2 wt% and 4 wt%).

Figures 7 and **8** show the physical and electrical properties of $0.99(Bi_{0.5}Na_{0.5})TiO_3$–$0.01Ba(Zr_{0.04}Ti_{0.96})O_3$ ceramics with different Bi_2O_3 addition sintered at 1100°C for 2 h. The measured density and dielectric constant of 0.99NBT–0.01BZT ceramics sintered 1100°C are shown as a function of Bi_2O_3 addition in Fig. 7. The measured density and dielectric constant of 0.99NBT–0.01BZT ceramic increase with increasing Bi_2O_3 addition until it reaches 0.5 wt%, then decrease above 0.5 wt%. The planar coupling factor (k_p) and thickness coupling factor (k_t) of 0.99NBT–0.01BZT ceramic are shown as function of Bi_2O_3 addition in Fig. 8. The planar coupling factor (k_p) increases with increasing Bi_2O_3 addition until it reaches 0.5 wt%, then decreases above 0.5 wt%. The thickness coupling factor (k_t) increases with increasing Bi_2O_3 addition until it reaches 0.5 wt%, then decrease above 0.5 wt%. For 0.99NBT–0.01BZT ceramic with the addition of 0.5 wt% Bi_2O_3, the electromechanical coupling coefficients of the planar mode k_p and the thickness mode k_t reach 0.15 and 0.54, respectively, at the sintering of 1100°C for 2 h. The ratio of thickness coupling coefficient to planar coupling coefficient is 3.6.

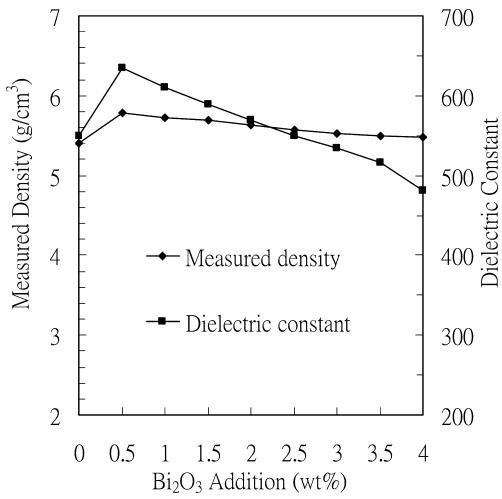

Fig. 7. Dielectric constant and measured density of $0.99(Bi_{0.5}Na_{0.5})TiO_3$–$0.01Ba(Ti_{0.96}Zr_{0.04})O_3$ ceramics sintered 1100°C for 2 h as a function of Bi_2O_3 addition.

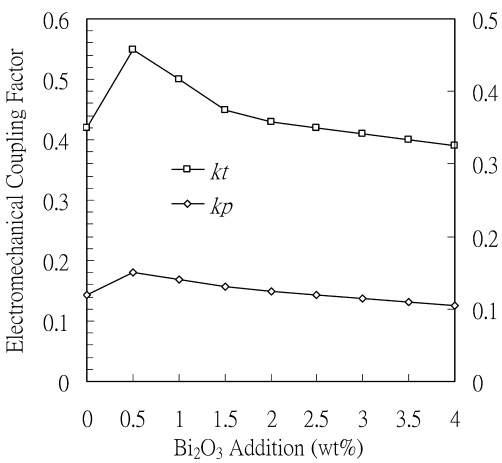

Fig. 8. Thickness coupling factor and planar coupling factor of $0.99(Bi_{0.5}Na_{0.5})TiO_3$–$0.01Ba(Ti_{0.96}Zr_{0.04})O_3$ ceramics sintered 1100°C for 2 h as a function of Bi_2O_3 addition.

Figure 9 shows the microstructure of $0.99(Na_{0.5}Bi_{0.5})TiO_3$–$0.01Ba(Zr_{0.04}Ti_{0.96})O_3$ ceramics sintered at 1100°C for different time: (a) 2 h, (b) 5 h, and (c) 8 h. It can be seen that the 0.99NBT–0.01BZT ceramic consists of very small grains, with a relatively loose structure, and a high porosity in Fig. 9(a). However, the 0.99NBT–0.01BZT ceramic for 5 h of the sintering time at 1100°C is more dense, with low porosity, and exhibits a more homogeneous and grain size of ~1.5 μm in Fig. 9(b). It may be explained by the sintering model of Coble[13] that small grain size will promote the densification and grain boundary offer a sink of defect or vacancy in sintering leading to the increase of the density. In Fig. 9(c), the porosity is increased. Increasing the porosity attributed to a greater rate of evaporation of Bi_2O_3 compared to that recondensed. **Figure 10** shows the SEM images of

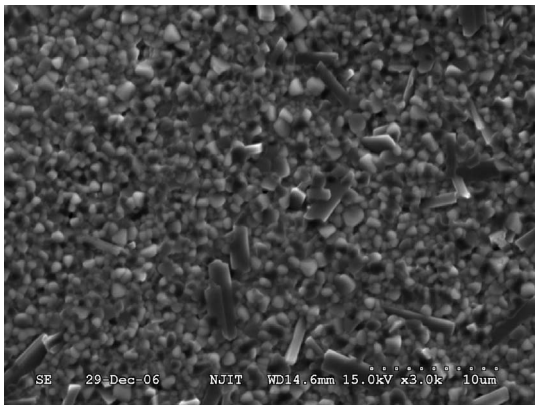

(a) 2 h

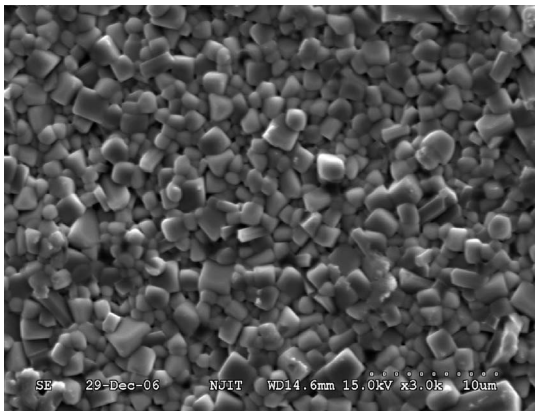

(b) 5 h

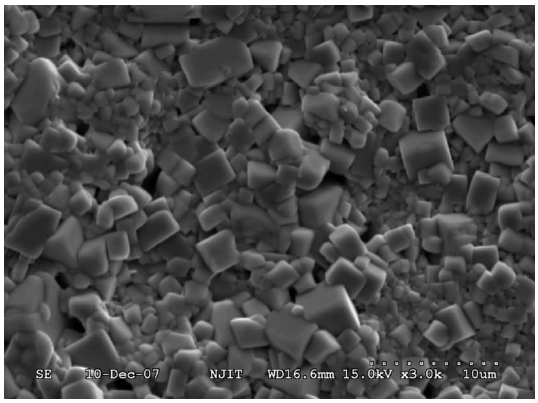

(c) 8 h

Fig. 9. SEM images of $0.99(Bi_{0.5}Na_{0.5})TiO_3$–$0.01Ba(Ti_{0.96}Zr_{0.04})O_3$ ceramics sintered at 1100°C for different time: (a) 2 h, (b) 5 h, and (c) 8 h.

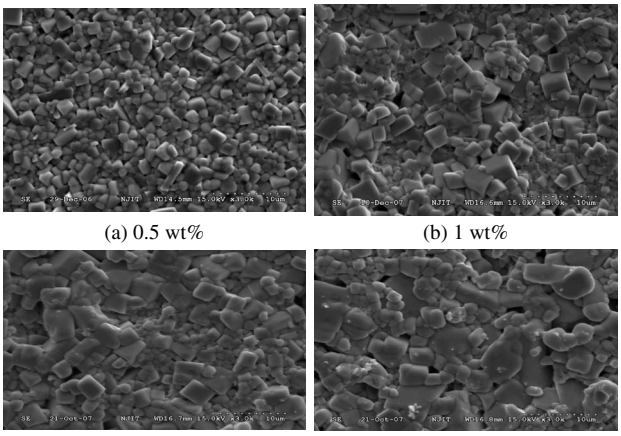

(a) 0.5 wt% (b) 1 wt%

(c) 2 wt% (d) 4 wt%

Fig. 10. SEM images of $0.99(Bi_{0.5}Na_{0.5})TiO_3$–$0.01Ba(Ti_{0.96}Zr_{0.04})O_3$ ceramics sintered at 1100°C for 2 h with different Bi_2O_3 addition: (a) 0.5 wt%, (b) 1 wt%, (c) 2 wt%, and (d) 4 wt%.

Table 2. Physical and Electric Properties of $0.99(Bi_{0.5}Na_{0.5})TiO_3$–$0.01Ba(Ti_{0.96}Zr_{0.04})O_3$ with Excess Bi_2O_3 Addition at the Sintering of 1100°C

Sintering time	Excess Bi_2O_3 addition	Relative density	Grain size (μm)	$K^T{}_{33}$	k_p	k_t	k_t/k_p
8 h	0	91.8%	2.5	570	0.13	0.48	3.7
5 h	0	93.5%	1.5	758	0.14	0.51	3.6
2 h	0	90.2%	0.5	550	0.12	0.42	3.5
2 h	0.5 wt%	96.5%	1.5	635	0.15	0.54	3.6
2 h	1.0 wt%	95.5%	2.0	610	0.14	0.5	3.6
2 h	2.0 wt%	93.9%	2.5	570	0.125	0.44	3.5

$0.99(Na_{0.5}Bi_{0.5})TiO_3$–$0.01Ba(Zr_{0.04}Ti_{0.96})O_3$ ceramics with different Bi_2O_3 addition sintered at 1100°C for 2 h. It is evident that Bi_2O_3 addition causes a significant change in the grain size. It seems that Bi_2O_3 addition enhances the grain growth. However, at the addition more than 1 wt%, the porosity is increased. Increasing the porosity will degrade properties of the ceramic body.

Table 2 shows the physical and electrical properties of $0.99(Na_{0.5}Bi_{0.5})TiO_3$–$0.01Ba(Zr_{0.04}Ti_{0.96})O_3$ ceramic with excess Bi_2O_3 addition at the sintering of 1100°C. The relative density is the ratio of the measured density to the theoretical density. The relative density and the grain size of 0.99NBT–0.01BZT ceramic without excess Bi_2O_3 addition is 90.2% and 0.5 μm, respectively, for 2 h of the sintering time at 1100°C. Prolonged the sintering time to 5 h, the relative density was raised to 93.5% and the grain size was increased to 1.5 μm. In this system, the properties have better values for 5 h of the sintering time at 1100°C. From the XRD patterns observation, a longer sintering time causes excessive Bi_2O_3 loss and a resultant variation in composition, which leads to an inhomogeneous microstructure. In Fig. 9(c), the porosity is increased. Increasing the porosity may be attributed to a greater rate of evaporation of Bi_2O_3 compared to that recondensed. With further increasing the sintering time to 8 h, the porosity of 0.99NBT–0.01BZT ceramic increases as shown in Fig. 9(c), and the properties diminish gradually. The 0.99NBT–0.01BZT ceramic with 0.5 wt% Bi_2O_3 addition has more dense structures and better properties than without the addition of excess Bi_2O_3. The relative density was raised to 96.5% and the grain size was increased to 1.5 μm for the 0.99NBT–0.01BZT ceramic with 0.5 wt% Bi_2O_3 addition. The addition of excess Bi_2O_3 to the 0.99NBT–0.01BZT system is a promising approach to improve densification and properties, as it may compensate for loss during sintering or aid densification by formation of a liquid phase. A small amount of the second phase appears for higher Bi_2O_3 addition, as shown in Figs. 6(c) and 6(d). The second phase was considered as a Bi_2O_3 phase, which degraded properties of the ceramic body.

4. Conclusion

The $(1-x)(Na_{0.5}Bi_{0.5})TiO_3$–$xBa(Zr_{0.04}Ti_{0.96})O_3$ solid solution ceramics were prepared by the conventional ceramic sintering technique. For 0.99NBT–0.01BZT ceramic, the electromechanical coupling coefficients of the planar mode k_p and the thickness mode k_t reach 0.14 and 0.51, respectively, at the sintering of 1100°C for 5 h. The ratio of thickness coupling coefficient to planar coupling coefficient is 3.6.

The effects of sintering time and Bi_2O_3 addition on the properties of 0.99NBT–0.01BZT ceramic were discussed. For 0.99NBT–0.01BZT ceramic with the addition of 0.5 wt% Bi_2O_3, the electromechanical coupling coefficients of the planar mode k_p and the thickness mode k_t reach 0.15 and 0.54, respectively, at the sintering of 1100°C for 2 h. The ratio of thickness coupling coefficient to planar coupling coefficient is 3.6. The addition of excess Bi_2O_3 and prolonging the sintering time to the 0.99NBT–0.01BZT system are two helpful methods on ceramic processing to improve densification and properties. Our results show that 0.99NBT–0.01BZT solid solution ceramic are one of the promising lead-free ceramics for high frequency electromechanical transducer applications.

Acknowledgement The author would like to acknowledge the financial support of the National Science Council (under contract NSC–96–2215–E–232–002) of the Republic of China.

References

1) G. A. Smolensky, V. A. Isupov, A. I. Agranovskaya, N. Krainik and N. Fizika, *Sov. Phys.-Solid State (Engl. Transl.)*, 2, 2651–2654 (1961).
2) T. Takenaka, K. Sakata and K. Toda, *Ferroelectric*, 106, 375–380 (1990).
3) T. Takenaka, K. Maruyama and K. Sakata, *Jpn. J. Appl. Phys.*, 30, 2236–2239 (1991).
4) A. Herabut and A. Safari, *J. Am. Ceram. Soc.*, 80, 2954–2958 (1997).
5) T. Takenaka and H. Nagata, *Jpn. J. Appl. Phys.*, 36, 6055–6057 (1997).
6) N. Ichinose and K. Udagawa, *Ferroelectric*, 169, 317–325 (1995).
7) A. Sasa, T. Chiba, Y. Mamiya and E. Otsuki, *Jpn. J. Appl. Phys.*, 38, 5546–5567 (1999).
8) C. H. Wang, *Jpn. J. Appl. Phys.,* 41[8], 5317–5322 (2002).
9) C. H. Wang, *J. Ceram. Soc. Japan*, 116[5], 632–636 (2008).
10) J. Hu and Z. Chen, *Key Eng. Mater.*, 368, 1915–1918 (2008).
11) Anon., *Proc. IRE.*, 49, 1161–1168 (1961).
12) T. Senda and R. C. Bradt, *J. Am. Ceram. Soc.*, 73[1], 106 (1990).
13) R. L. Coble, *J. Appl. Phys.*, 56, 131–141 (1985).
14) E. G. Fesenko, A. Y. Dantsiger, L. A. Resnitohenko and M. F. Kupriyanov, *Ferroelectrics*, 41, 137–141 (1982).
15) K. Okazaki and K. Nagata, *J. Am. Ceram. Soc.*, 56[2], 82–86 (1973).
16) K. H. Hartal, *Ferroelectrics*, 12, 9–19 (1976).